

Research Article

Mathematical Simulation of Lost Circulation in Fracture and Its Control

Xiao Cai ¹, Boyun Guo,² Qingfeng Guo,¹ and Hongwei Jiang¹

¹CNPC Engineering Technology R&D Company Limited, China

²University of Louisiana at Lafayette, USA

Correspondence should be addressed to Xiao Cai; caixiaodr@cnpc.com.cn

Received 16 December 2020; Revised 28 January 2021; Accepted 4 February 2021; Published 12 March 2021

Academic Editor: Amgad Salama

Copyright © 2021 Xiao Cai et al. This is an open access article distributed under the Creative Commons Attribution License, which permits unrestricted use, distribution, and reproduction in any medium, provided the original work is properly cited.

Lost circulation has been one of the major problems that impede efficient and cost-saving drilling operations. The nature of lost circulation and its control is not yet fully understood. A method to characterize the mud loss in fracture and the plugging process of lost circulation materials is highly desired to obtain a thorough understanding of mud losses in fracture and provide reference for lost circulation control. This paper presents an easy-to-use method to identify types of lost circulation in fracture and the corresponding control. Three analytical models are presented based on three loss mechanisms, namely, seepage/filtration in a fracture, pipe flow in a fracture, and gravity displacement in a fracture. A numerical model is developed to simulate the deposition of lost circulation materials in fractures and predict the time and the volume of drilling fluid needed for lost circulation control. Case studies with these analytical models provide a deeper insight of this subject. Sensitivity analyses with the numerical model identify the major factors responsible for lost circulation control. High viscosity of drilling fluid may prevent lost circulation, while low viscosity is desired for a fast control of lost circulation. Lowering the density of drilling fluid is another way to prevent the lost circulation and facilitate the deposition of lost circulation materials. Lost circulation materials with high density could deposit faster close to the wellbore and therefore accelerating the control process. High concentration of lost circulation materials is likely to shorten the plugging time, which should be determined referring to the severity of loss. This work provides drilling engineers a practical method for simulating the lost circulation and selecting lost circulation material.

1. Introduction

Lost circulation is a condition that the drilling fluid uncontrollably flows into the formation instead of returning back to the surface while drilling a well. In addition to the loss of drilling fluid, lost circulation may decrease the bottom hole pressure, which will lead to well control [1] and wellbore instability issues (collapse). Besides, lost circulation may result in dry drilling (a condition that drilling fluid is totally lost from the wellbore), which will greatly damage the drill bit and the wellbore. Cost overruns will be generated by the loss of material and loss of productive time. Worldwide, the lost circulation leads to annual 2-4 billion dollars loss due

to decreased productive time, lost drilling fluid, and materials used to prevent the loss [2].

Many researchers have investigated the mathematical models of lost circulation. Majidi et al. [3, 4] presented a model of non-Newtonian drill mud loss in naturally fractured formation based on the principles of conservation of mass and linear momentum for drilling fluid and pressure diffusion for reservoir fluid. Majidi et al. (2010) proposed a quantitative analysis of mud loss in naturally fractured reservoirs considering the rheology properties of drill mud. They opined that the mud loss could be minimized by optimizing the rheology of drill mud such as the yield stress and shear-thinning/-thickening effect. Li

et al. [5] established a lost circulation pressure model suitable for different lost circulations in carbonate formations based on leakage mechanisms. Wang et al. [6] developed a numerical simulation to investigate drilling fluid loss in fractured formations considering fracture wall roughness. Feng and Gray [7] proposed a numerical model considering the actual condition of dynamic mud circulation and the induced-fracture propagation in the drilling process to estimate the rate of loss and fracture profile.

Due to the serious consequences of lost circulation, numerous methods and techniques have been developed to prevent and remediate the issue and thereby minimize the drilling cost. Sanders et al. [8] proposed a new high-fluid-loss and high-strength lost circulation system to address the lost circulation. Castro et al. [9] introduced an application of heat-activated and rigid rapid-fluid system to deal with the severe loss of circulation in deep-water environment and expand the gradient window. Ay et al. [10] developed an environmentally friendly silicate-polymer gel system with adjustable viscosity and density to seal shallow water flow and lost circulation in top hole drilling. Zhao et al. [11] presented a fully coupled hydraulic fracturing model based on the cohesive zone model, which describes the dynamic process of fracture growth and wellbore behavior during lost circulation. Mehrabian and Abousleiman [12] presented a wellbore-stability analysis of a fractured and LCM-treated wellbore. Abdila et al. [13] introduced a successful application of casing drilling technique to solve the issue of losses in the Louise fields, demonstrating its benefits of wellbore strengthening and efficiency improvement. Hou et al. [14] did a pioneering work to forecast lost circulations in south China sea by using an artificial neural network model. Pazziuagan et al. [15] highlighted a geomechanics modeling software to prevent lost circulation in offshore wells with narrow pressure margin and depleted reservoir.

Lost circulation materials are commonly used in strengthening the wellbore and thereby remediate the lost circulation by bridging, plugging, or sealing the fractures, where the lost circulation occurs [7, 16]. A number of studies on LCM materials to mitigate the lost circulation condition have been proposed. Kefi et al. [17] proposed a novel composite blend system for controlling lost circulation based on a new four-step methodology. Javeri et al. [18] proposed a method of using silicon nanoparticles in drilling fluid to form a more integrated and thinner mud cake for mitigating lost circulation and differential sticking problems. Guo et al. [19] performed an investigation of mitigating lost circulation of oil-based drilling fluids by using gilsonite. Savari et al. [20] determined the plug-breaking pressure of different LCM combinations based on a permeability-plugging apparatus with tapered slots to evaluate their ability to experience displacement and failure pressures. Razavi et al. [21] proposed a method to determine the optimal LCM particle size distribution for LCM blend, which can maximize the wellbore strengthening effect obtained from fracture sealing. Nasiri et al. [22] used an advanced experimental method to determine the effectiveness of various LCMs on loss control in bentonite mud. Kulkarni et al.

[23] performed an experimental study to evaluate the suspension characteristics of lost-circulation materials in different drilling fluids and analyzed the effects of suspending agents. Jaffery et al. [24] proposed an engineered fiber-based lost circulation control pills based on special fiber system and particle size distribution principle to solve the lost circulation challenges in a depleted formation with natural fractures. Xu et al. [25] experimentally analyzed the effects of multiple factors, such as low rate, particle size distribution, and particle geometry, on the transport and captured characteristics of lost circulation material. Savari and Whitfill [26] provided three types of lost circulation materials which were demonstrated by case studies to be efficient to manage severe losses of circulation. In 2020, a high fluid loss squeeze and reticulated foam lost circulation material is provided by Savari to deal with serious losses in naturally fractured/vugular formations with supporting data of experimental tests. Feng et al. [27] illustrated a novel method to inject the lost circulation materials, which is named as graded multiple injection method and proposed a visualization experimental means to support their conclusions.

For the simulation of fluid loss, previous models assumed the pipe flow of single-phase liquid in fractures, while the seepage flow (filtration) and gravity displacement in the fractures have not been studied. This paper proposed three analytical models to individually simulate different types of lost circulation processes considering the seepage flow, pipe flow, and gravity displacement in fracture. Previous works mainly focus on the improvement of LCM to prevent and mitigate the lost circulation condition. No studies so far can provide a description of the LCM particle transport in the fracture and give out a time at which the fracture is completely sealed. This paper fills the gap by providing a numerical model to simulate the sealing process of LCMs in fracture and predict the time for controlling the lost circulation as well as the volume for curing the well.

2. Mathematical Model

In the case of lost circulation caused by fractures, the drill mud flowing in fracture can be generally characterized by fluid filtration, pipe flow, and gravity displacement in fracture. A simple method to identify the type of losses for LCM selection and predict the losses is highly desired. In order to elaborate the lost circulations caused by fractures, three analytical models are derived to simulate three loss conditions in fracture. A numerical model is presented to simulate the curing processes.

2.1. Analytical Models for Diagnosis of Types of Lost Circulation

2.1.1. Loss of Circulation due to Fracture Seepage Flow. Darcy's law applies in the liquid seepage/filtration in a fracture depicted in Figure 1. The loss rate in Darcy's units is expressed as (see Appendix A for derivation):

$$q = 2wh_f v = \sqrt{2c_k} wh_f t^{-1/2}, \quad (1)$$

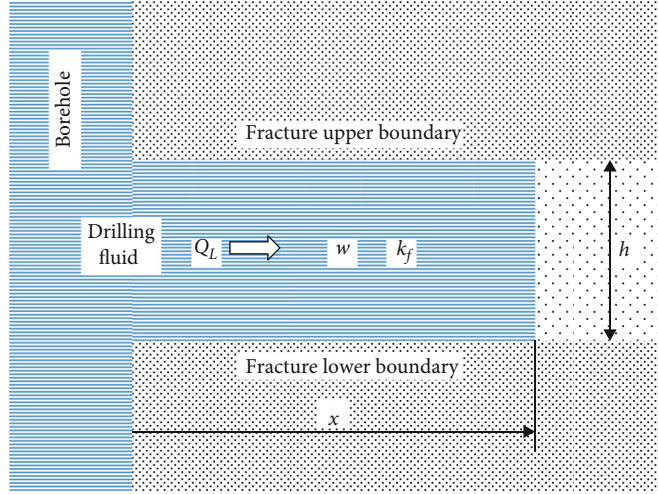


FIGURE 1: Cross-sectional view of liquid seepage in a fracture.

where q is the total loss rate from two wings of a linear fracture, w is fracture width, h_f is fracture height, t is time, and c_k is defined as

$$c_k = \frac{k_f(p_w - p_f)}{\mu}, \quad (2)$$

where k_f is fracture permeability, μ is drilling fluid viscosity, and p_w and p_f are pressures in the wellbore and fracture, respectively.

The cumulative volume of lost fluid is expressed by:

$$V_L = 2wh_f x = 2\sqrt{2c_k} wh_f t^{1/2}. \quad (3)$$

2.1.2. Loss of Circulation due to Fracture Pipe Flow. Figure 2 shows the liquid pipe flow in a fracture. Darcy's law does not apply to the liquid pipe flow. Friction factor dominates loss rate and the expression for the loss rate in SI units is (see Appendix A for derivation)

$$q = \frac{4}{3} \left(\frac{3}{2} c_f \right)^{2/3} wh_f t^{-1/3}, \quad (4)$$

where

$$c_f = \sqrt{\frac{h_f(p_w - p_f)}{\pi f \rho_L}}, \quad (5)$$

where ρ_L is liquid density and f is friction factor.

The cumulative volume of lost liquid is expressed as

$$V_L = 2 \left(\frac{3}{2} c_f \right)^{2/3} wh_f t^{2/3}. \quad (6)$$

2.1.3. Loss of Circulation due to Gravity Displacement. For steady liquid intrusion into a fracture due to gravity segregation

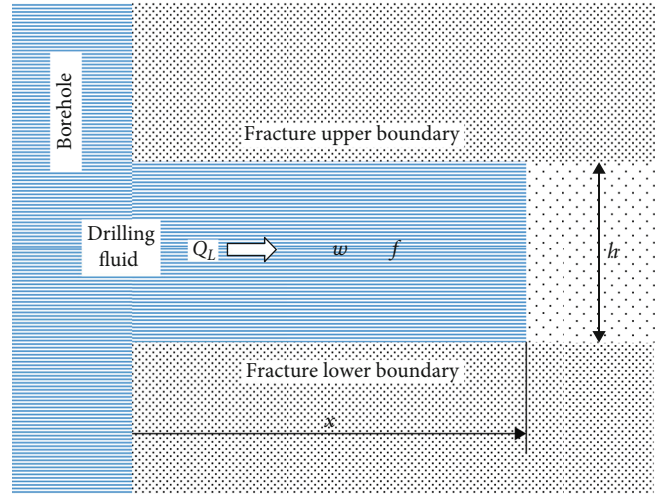


FIGURE 2: Cross-sectional view of liquid pipe flow in a fracture.

tion depicted in Figure 3, an analytical model was derived. Model derivation is shown in the Appendix A. The loss rate in SI units is expressed as

$$q = \frac{w}{\rho_L^2 \sqrt{\pi g^3 f L_f}} (p_w - p_f)^2, \quad (7)$$

where g is gravitational acceleration and L_f is travel distance of the liquid front propagating in the fracture (it is also referred as the fracture length invaded by the liquid). The cumulative volume of lost liquid can be calculated based on numerical integration of Equation (7) over time.

2.2. Numerical Model for Curing Lost Circulation. For the remedial treatment, it is highly desirable to figure out the time for lost circulation control and thus the total volume of drilling fluid needed. In this study, a new mathematical model is developed to predict the location of LCMs and the plugging time for lost circulation control. Figure 4 shows a

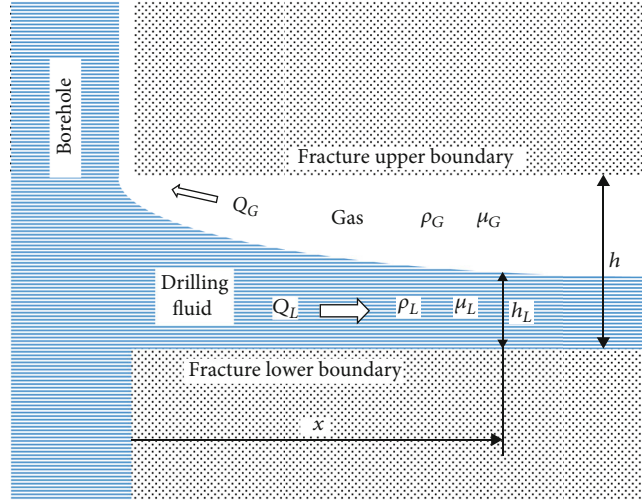


FIGURE 3: Cross-sectional view of liquid flow in a fracture due to gravity displacement.

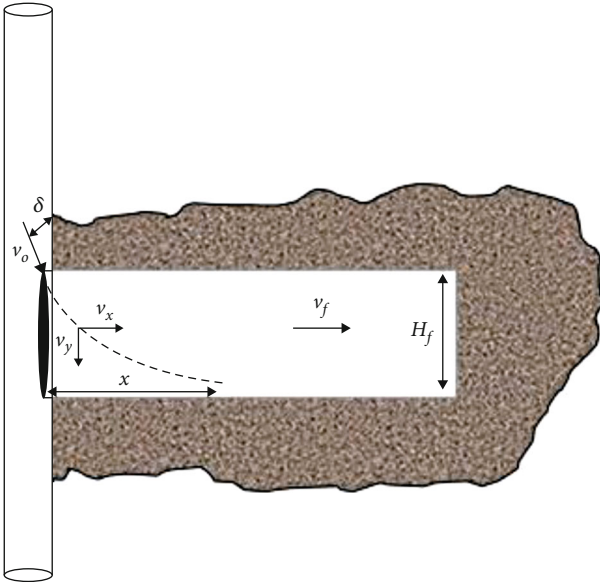


FIGURE 4: Trajectory of LCM particle flowing inside a fracture.

sketch of single LCM particle flowing into the fracture with an inclination angle of δ , where v_o is the initial velocity of particle, v_x and v_y represent the velocity components in the vertical and horizontal directions, respectively.

The settling distance of LCM particle is (see Appendix B for derivation)

$$y = \frac{1}{\beta} \sqrt{W-B} \left[t + \frac{2}{\alpha} \ln \left(\frac{C_y + e^{-\alpha t}}{C_y + 1} \right) \right], \quad (8)$$

where

$$\alpha = \frac{2g_c\beta}{m_m} \sqrt{W-B}, \quad (9)$$

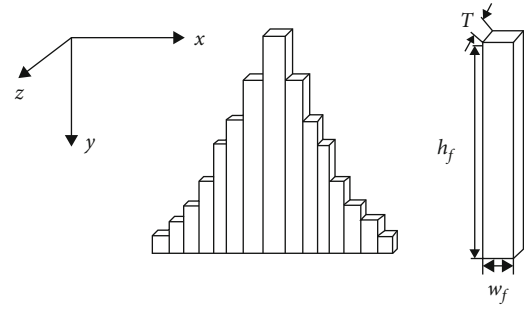


FIGURE 5: A sketch of the rectangular-slice model and a single LCM slice.

$$\beta = \sqrt{\frac{fA\rho_f}{2g_c}}, \quad (10)$$

$$C_y = \frac{\sqrt{W-B} + v_{yo}\beta}{\sqrt{W-B} - v_{yo}\beta}. \quad (11)$$

W is the LCM particle weight, lbf; B is the buoyant force, lbf. They are defined as:

$$W = \frac{g}{g_c} \rho_m V_m, \quad (12)$$

$$B = \frac{g}{g_c} \rho_f V_m, \quad (13)$$

where m_m is the LCM mass, f is the friction factor, ρ_f is drilling fluid density, ρ_m is the LCM density, A is the characteristic area of particle, v_{yo} initial velocity of LCM particle in y -direction, V_m is the volume of LCM particle, g_c is the unit conversion factor, which is 32.17 (ft-lb_m/lb_f-s²).

The traveling distance of LCM particle is expressed as

$$x = v_L t + \frac{2m_m}{fA\rho_f} \ln \left(\frac{C_x}{t + C_x} \right), \quad (14)$$

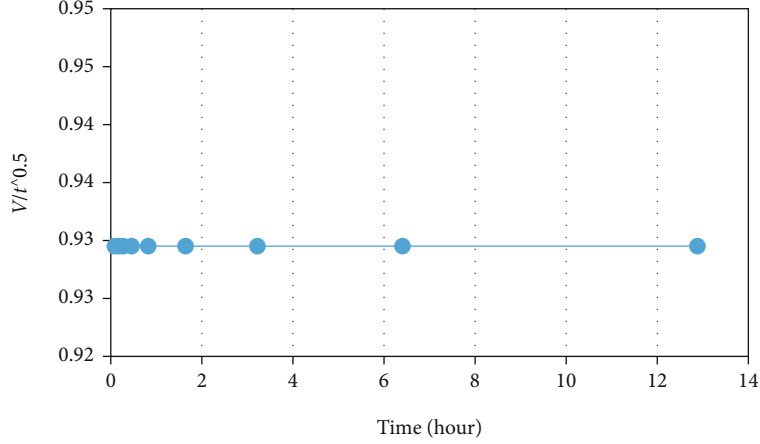


FIGURE 6: Plot of lost volume data divided by the square root of time versus time showing a data trend of zero slope.

where

$$C_x = \frac{2m_m}{fA\rho_m(v_L - v_{xo})}. \quad (15)$$

v_L is the fracturing fluid velocity, v_{xo} is the initial LCM particle velocity in x -direction, m_m is the LCM particle mass, lbm, f is the friction factor, ρ_f is drilling fluid density, and A is the characteristic area of LCM particle.

Set the settling distance in the vertical direction in Equation (8) to be the fracture height, the settling time is expressed as

$$t = -\frac{2}{\alpha} \ln \frac{(C_y + 1)e^{(\alpha/2)(H_f\beta/\sqrt{W-B})} + \sqrt{(C_y + 1)^2 e^{\alpha(H_f\beta/\sqrt{W-B})} - 4C_y}}{2}. \quad (16)$$

When the LCM particles flow into the fracture, pile of LCM will form in the fracture. In order to mathematically simulate the forming process of the LCM pile, it is considered as an integration of rectangular pile elements. Figure 5 is a sketch of rectangular-slice model and single slice of LCM pile. The volume of slice i , which is composed of LCM particles of size d_{mi} , can be expressed as

$$V_i = f_{Vi}V_t, \quad (17)$$

where f_{Vi} is the volume fraction of LCM with size d_{mi} , V_i is the volume of the slice composed of the LCM of size d_{mi} , and V_t is the total volume of LCM pile.

The volume of slice i containing the LCM of size d_{mi} is formulated as

$$V_i = \omega_i h_i T_i, \quad (18)$$

where ω_i is the width of slice composed of LCM with size d_{mi} , which is assumed to be the fracture width; h_i is the height of slice containing LCM of size d_{mi} ; T_i is the thickness of slice composed of the LCM of size d_{mi} .

TABLE 1: Fluid and fracture properties for model analysis.

Well depth (D)	3000	m
Liquid density (ρ_L)	1400	kg/m ³
Liquid viscosity (μ)	5	cp
Fracture height (h_f)	500	cm
Fracture width (w)	1	cm
Fracture permeability (k_f)	10	Darcy
Pore pressure gradient (G_p)	0.12	Atm/m

The thickness of the slice composed of LCM of size d_{mi} can be expressed as

$$T_i = x_i - x_{i+1}, \quad (19)$$

where x_i is the horizontal drifting distance of LCM with size d_{mi} and x_{i+1} is the horizontal drifting distance of LCM with size d_{mi+1} .

The height of pile slice containing the LCM of size d_{mi} can be expressed as

$$h_i = \frac{V_i}{\omega_i T_i}. \quad (20)$$

The configuration of LCM pile in fracture is the integration of pile element.

2.3. Model Analysis. The procedure of applying the proposed method includes 3 steps:

- (i) Step 1: identify the mechanism of loss of circulation. During application, first, we need to identify the type of lost circulation. Identification of the loss mechanisms can be made by plotting the lost volume data from pit loss measurement. For the seepage type of lost circulation, the cumulative lost volume of drilling fluid is proportional to the square root of time. This means that the relationship between the pit loss data divided by the square root of time versus the

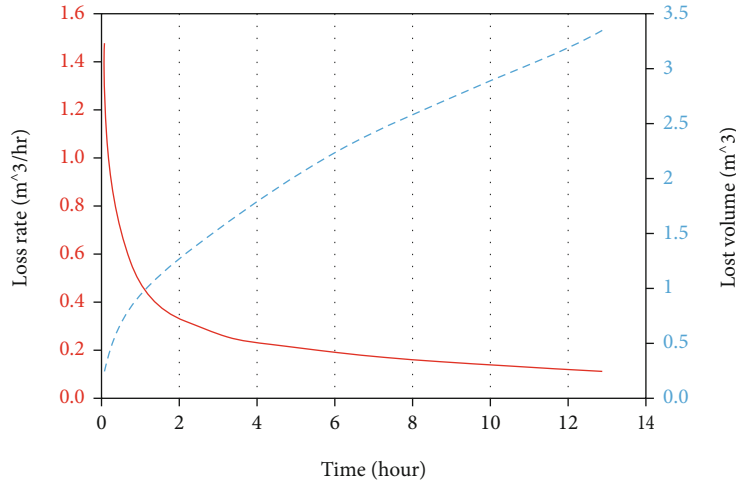


FIGURE 7: The trends of loss rate and cumulative volume for seepage type of lost circulation.

time should show a zero-slope trend. Besides, the lost circulation due to gravity displacement also shows a zero-slope trend between the lost volume of drilling fluid divided by time versus time. However, the gas or oil cut in the drilling fluid can explicitly demonstrate a lost circulation of gravity displacement type. Therefore, the lost circulation is characterized as the fracture pipe flow, when the plot of lost volume of drilling fluid divided by the square root of time versus time does not show a data trend of zero-slope

- (ii) Step 2: predict the loss rate and volume of drilling fluid at a given time using the corresponding lost circulation model
- (iii) Step 3: predict the time of lost circulation control and the lost volume of drilling fluid used to control the lost circulation based on the proposed model

The lost circulation models are validated using the field data and experimental data obtained from a real size testing setup. The field pit loss data divided by the square root of time versus time is plotted in Figure 6, demonstrating a trend of zero slope. The zero slope of the plot shown in Figure 6 indicates a fact that the lost circulation is due to the fracture seepage flow. After identifying the type of lost circulation, the loss flow rate and lost volume of drilling fluid can be predicted based on the corresponding model. The model for lost circulation due to fracture seepage flow is validated using the data shown in Table 1. Figure 7 shows the trends of loss rate calculated by Equation (1) and cumulative volume calculated by Equation (3). The rapid decline in loss rate indicates that there is no need to use high concentrations of LCM to control the lost circulation.

The other two lost circulation models were validated with the experimental data shown in Table 2 obtained from a real size testing setup, which is described elsewhere.

TABLE 2: Geometry and operating conditions in an experimental test.

Liquid density (ρ_L)	1000	kg/m ³
Liquid viscosity (μ)	5	cp
Fracture height (h_f)	0.7	m
Fracture width (w)	0.1	cm
Invaded fracture length (L_f)	1.2	m
Borehole pressure (p_w)	15	kPa
Fracture pressure (p_f)	10	kPa

The profiles of loss rate and cumulative volume calculated by the fracture pipe flow model using the data in Table 2 are presented by Figure 8. A rapid decline in loss rate is observed by the model. However, the high sustainable loss requires the use of high concentrations of LCM.

Figure 9 represents a graph of the trends of loss rate and cumulative volume using the gravity displacement model. High concentration of LCM is suggested because a slow decline in loss rate is illustrated by the model.

The plugging model is validated using the fluid and fracture properties in Table 1 and the properties of LCM in Table 3. Size distribution of LCM is shown in Table 4. After 6.42 hours, the lost circulation is controlled; the volume of lost circulation is 9.44 m³. Figure 10 demonstrates the final configuration of LCM pile in fracture, which totally seals the fracture.

2.4. Sensitivity Analysis. To minimize drilling cost, it is highly desirable to figure out factors that affect the plugging time and the lost volume of drilling fluid. In this study, sensitivity analysis was performed with the proposed numerical model to identify the major factors responsible for the lost circulation using the data in the case study with one parameter value changed at a time.

Figure 11 shows the time of controlling the lost circulation using different viscosities of drilling fluid. Increasing

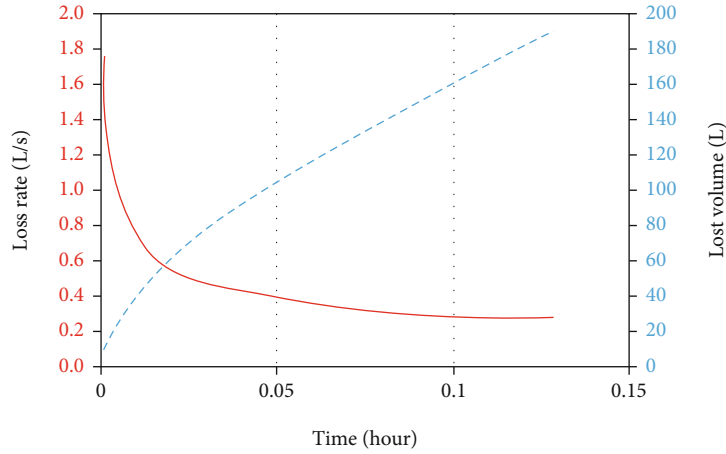


FIGURE 8: The trends of loss rate and cumulative volume for pipe flow type of lost circulation.

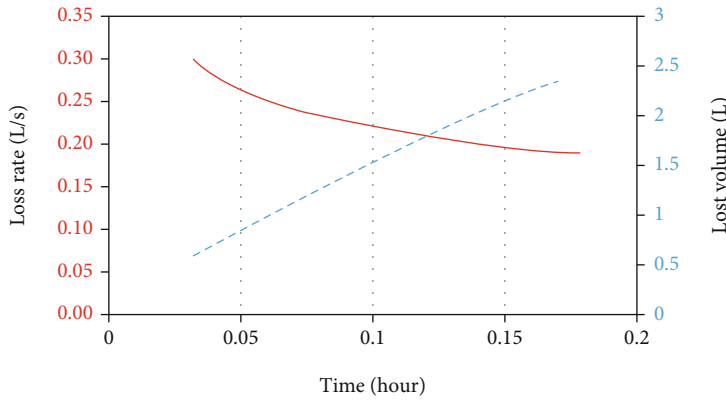


FIGURE 9: The trends of loss rate and cumulative volume for gravity displacement type of lost circulation.

TABLE 3: Properties of LCM used in case study.

Parameter	Value	Unit
Drilling fluid lost rate	1.4697	m ³ /h
LCM density	1650	kg/m ³
LCM sphericity	0.82	
Number of fracture	1	
LCM discharge angle	45	Degree
Ratio of LCM to drilling fluid	0.05	
Number of injection point	1	

TABLE 4: Side distribution of lost circulation material.

Mesh	μm	Fraction %
100	149	8.36
60	250	10.33
40	420	32.86
20	840	29.48
16	1190	17.14
12	1680	1.26
8	2380	0.57

the viscosity of drilling fluid is one of the major ways to prevent lost circulation by enhancing the filter cake (Liu, 2008; Deng, 2008). The proposed analytical models for simulating the lost circulation also indicate that the loss rate can be reduced by increasing the viscosity of drilling fluid. However, increasing the viscosity of drilling fluid allows more LCM to stay in the annulus and increases the settling time of LCM in fracture. As a result, the time for completely controlling the lost circulation increases. Therefore, it is better to decrease the viscosity of drilling

fluid when LCM is added in the fracturing fluid to seal the fractures.

High density of drilling fluid creates a high mud pressure which can also cause the loss of circulation; therefore, reducing the density is another way to deal with the loss of circulation (Liu, 2008), which is consistent with Figure 12. Reducing the density of drilling fluid can not only avoid generating a high mud pressure but also facilitate the deposition of LCM and thereby accelerate fracture sealing.

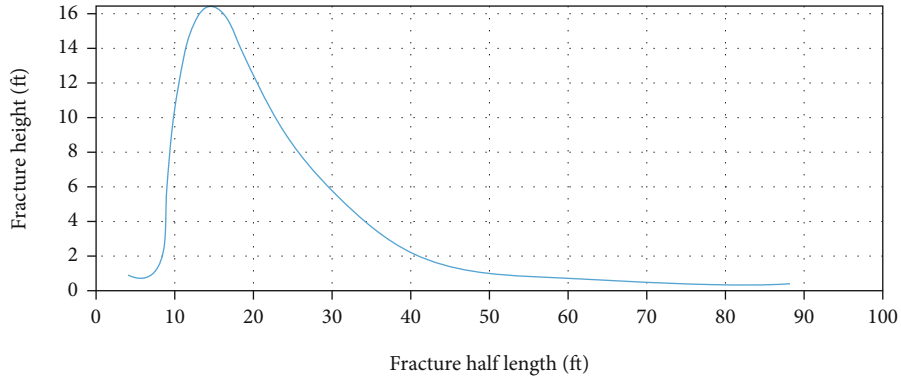


FIGURE 10: Configuration of LCM pile in fracture when the lost circulation is controlled.

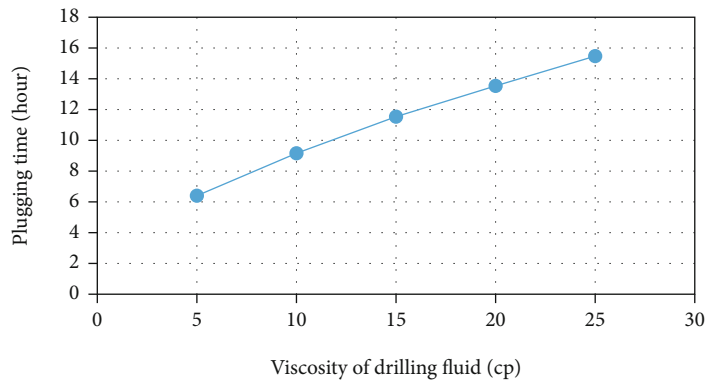


FIGURE 11: Plugging time versus viscosity of drilling fluid.

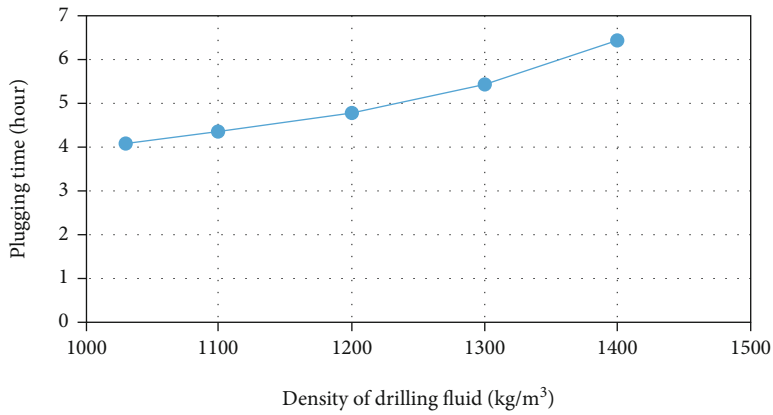


FIGURE 12: Plugging time versus density of drilling fluid.

Properties of LCM are also needed to be considered during bridging the fractures. Figure 13 presents the time for completing bridging the fracture using different LCM densities. LCM with high density can deposit in the mouth of fracture faster, forming a pile of LCM to plug the fracture and remediate the loss of circulation. Hence, LCM with higher density is preferred during curing the lost circulation.

The concentration of LCM is another important factor because it determines the amount of LCM within the drilling fluid entering the fracture. Figure 14 shows that increasing the concentration of LCM is more likely to shorten the time to plug the fracture face. The concentration of LCM should be determined based on the severity of lost circulation. A low concentration can be used to prevent the loss of circulation, and a high concentration is desired to mitigate the issue.

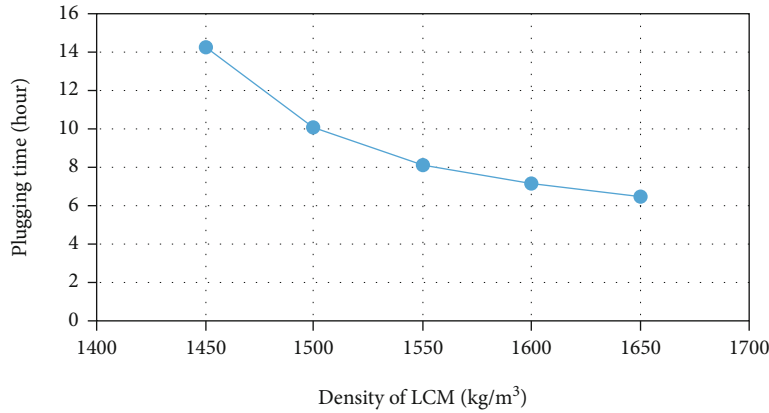


FIGURE 13: Plugging time versus density of LCM.

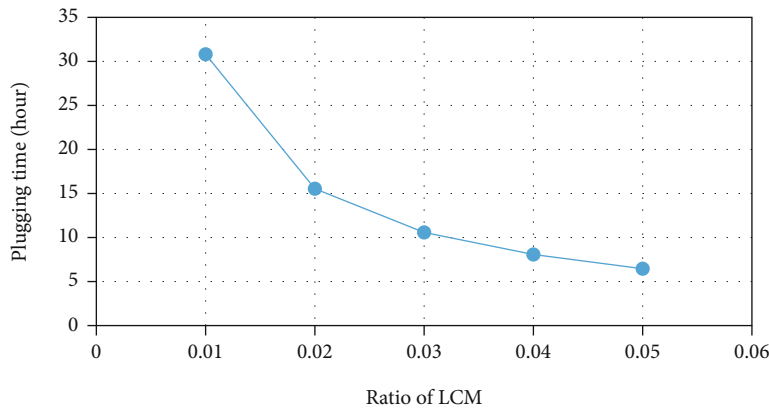


FIGURE 14: Plugging time versus ratio of LCM to fluid.

3. Conclusion

Three analytical models were developed to describe the lost circulation with three mechanisms in an inherently fractured reservoir or a reservoir with induced fracture. A simple method was used to identify the loss mechanisms. A numerical model was proposed to simulate the process of LCM deposition in fractures and predict the time for lost circulation control and the lost volume of drilling fluid. Case studies with these four models were conducted. Sensitivity analysis with the model for curing the lost circulation was performed. The following conclusions are drawn:

- (1) For the three types of loss of circulations, the loss rate can be reduced using drilling fluids of low density and high viscosity
- (2) Use of low fluid viscosity can control the lost circulation faster
- (3) Use of LCM with high density can facilitate the sealing process in fracture and reduce the time for controlling the lost circulation
- (4) Reducing mud density can mitigate the loss of circulation, but not as effective as the other factors investigated in this study

- (5) The concentration of LCM can determine the time needed to control the lost circulation; it should be selected based on the severity of lost circulation

Appendix

A. Derivation of Mathematical Models for Loss of Circulation

A.1 Loss of Circulation due to Fracture Seepage Flow. As depicted in Figure 1, the drilling fluid enters the fracture with a pressure p_w at the wellbore. Suppose the drilling fluid reaches a distance X in the fracture at time t , the pressure at the front of the fluid intrusion is the initial fracture pressure p_f . Fracture permeability can be assumed to be constant. Darcy’s law can be applied for liquid seepage/filtration in a fracture. Based on Darcy’s law, the governing equation for horizontal flow is expressed as

$$p_w - p_f = \frac{\mu}{k_f} X \frac{dX}{dt}, \tag{A.1}$$

where k_f is fracture permeability and μ is fluid viscosity.

Equation (A.1) can be simplified to

$$X \frac{dX}{dt} = c_k, \quad (\text{A.2})$$

where

$$c_k = \frac{k_f (p_w - p_f)}{\mu}. \quad (\text{A.3})$$

Integration of Equation (A.2) with the initial condition $X = 0$ at $t = 0$ yields

$$X = \sqrt{2c_k t^{1/2}}. \quad (\text{A.4})$$

The liquid velocity is obtained by taking derivative of this equation with respect to time, which is expressed as

$$v = \frac{\sqrt{2c_k}}{2} t^{-1/2}. \quad (\text{A.5})$$

Assuming two wings of a fracture are opened by the borehole, an expression for the total liquid seepage flow rate is obtained from Equation (A.5):

$$q = 2wh_f v = \sqrt{2c_k} wh_f t^{-1/2}. \quad (\text{A.6})$$

The cumulative volume of lost liquid for two wings is obtained from Equation (A.4):

$$V_L = 2wh_f x = 2\sqrt{2c_k} wh_f t^{1/2}. \quad (\text{A.7})$$

Equation (A.6) indicates that the loss rate of liquid is directly proportional to the fracture opening area wh_f for liquid seepage. However, these parameters are not controllable, Equation (A.3) suggests that pressure differential and fracture permeability should be lowered, and fluid viscosity should be increased to reduce loss of circulation.

A.2 Loss of Circulation due to Fracture Pipe Flow. Darcy's law does not apply to liquid pipe flow in a fracture depicted in Figure 2. While friction factor dominates loss rate, the governing equation for horizontal pipe flow is

$$p_w - p_f = \frac{2f\rho_L}{D_e} \left(\frac{dX}{dt} \right)^2 X, \quad (\text{A.8})$$

where the equivalent diameter of the fracture area can be estimated by $\pi D_e = 2h_f$, or

$$D_e = \frac{2h_f}{\pi}. \quad (\text{A.9})$$

Substituting Equation (A.9) into Equation (A.8) and rearranging the latter gives

$$\sqrt{X} \frac{dX}{dt} = c_f, \quad (\text{A.10})$$

where

$$c_f = \sqrt{\frac{h_f (p_w - p_f)}{\pi f \rho_L}}. \quad (\text{A.11})$$

Integration of Equation (A.10) with the initial condition $X = 0$ at $t = 0$ yields

$$X = \left(\frac{3}{2} c_f \right)^{2/3} t^{2/3}. \quad (\text{A.12})$$

Because the determination of the friction factor requires knowing liquid velocity, Equation (A.12) is taken derivative with respect to time giving

$$v = \frac{2}{3} \left(\frac{3}{2} c_f \right)^{2/3} t^{-1/3}. \quad (\text{A.13})$$

It is assumed that two wings of a fracture are opened by the borehole; the total liquid intrusion flow rate can be expressed by

$$q = 2wh_f v = \frac{4}{3} \left(\frac{3}{2} c_f \right)^{2/3} wh_f t^{-1/3}. \quad (\text{A.14})$$

The cumulative volume of lost liquid is obtained from Equation (A.12) for two wings:

$$V_L = 2wh_f x = 2 \left(\frac{3}{2} c_f \right)^{2/3} wh_f t^{2/3}. \quad (\text{A.15})$$

For laminar flow, the friction factor in Equation (A.11) is given by

$$f = \frac{16}{N_{\text{Re}}}, \quad (\text{A.16})$$

where the Reynolds number is defined by

$$N_{\text{Re}} = \frac{wv\rho_L}{\mu}, \quad (\text{A.17})$$

where μ is liquid viscosity. Because the friction factor is a function of Reynolds number which is a function of flow velocity which is a function of loss rate, the loss rate must be solved numerically.

A.3 Loss of Circulation due to Gravity Displacement. Figure 3 illustrates a steady liquid intrusion into a fracture due to gravity segregation. An analytical model can be obtained based on following assumptions:

- (1) Pipe flow exist in the fracture

- (2) Gas expansion is negligible due to minimal pressure variation in the fracture
- (3) Pressure variation of gas in the top side of the fracture is negligible due to the much lower viscosity of gas compared to liquid

Suppose the drilling fluid flows over a fracture length L_f , the pressures at the end of the fluid intrusion is the initial gas pressure p_f . The initial gas pressure p_f can be determined based on the pore pressure gradient and depth with negligible capillary pressure. Consider the liquid flow over a short interval dX at X distance from the wellbore, the governing equation for horizontal flow is

$$\frac{dp}{dX} = -\frac{2f\rho_L}{D_e} v^2, \quad (\text{A.18})$$

where the equivalent diameter of the fracture area is estimated by $\pi D_e = 2h_f$ or

$$D_e = \frac{2h_f}{\pi}. \quad (\text{A.19})$$

The fluid velocity can be estimated by

$$v = \frac{q_L}{wh_f}. \quad (\text{A.20})$$

Substituting Equations (A.19) and (A.20) into Equation (A.18) and rearranging the latter gives

$$\frac{dp}{dX} = -\frac{\pi f \rho_L q_L^2}{h_f^3 w^2}. \quad (\text{A.21})$$

The height of the liquid column in the fracture can be expressed as

$$h_L = \frac{p - p_f}{\rho_L g}. \quad (\text{A.22})$$

Substituting Equation (A.22) into Equation (A.21) and rearranging the latter result in

$$(p - p_f)^3 \frac{dp}{dX} = -\frac{\pi \rho_L^3 g^3 \rho_L f q_L^2}{w^2}, \quad (\text{A.23})$$

or

$$(p - p_f)^3 \frac{dp}{dX} = c_g, \quad (\text{A.24})$$

where

$$c_g = -\frac{\pi g^3 f \rho_L^4 q_L^2}{w^2}. \quad (\text{A.25})$$

Integrating Equation (A.24) gives

$$\frac{1}{4} (p - p_f)^4 = c_g X + C_1. \quad (\text{A.26})$$

Using boundary condition $p = p_w$ at $X = 0$, Equation (A.26) gives

$$C_1 = \frac{1}{4} (p_w - p_f)^4. \quad (\text{A.27})$$

Substituting Equation (A.27) into Equation (A.26) yields

$$p = p_f + \sqrt[4]{4c_g X + (p_w - p_f)^4}. \quad (\text{A.28})$$

The liquid flow rate into one fracture wing can be derived based on Equation (A.28) where X is set as L_f :

$$q_L = \frac{w}{2\rho_L^2 \sqrt{\pi g^3 f L_f}} (p_w - p_f)^2. \quad (\text{A.29})$$

The liquid flow rate into two fracture wings is expressed by

$$q = \frac{w}{\rho_L^2 \sqrt{\pi g^3 f L_f}} (p_w - p_f)^2. \quad (\text{A.30})$$

B. Derivation of LCM Particle Transport Model

The Newton's second law of motion indicates that the vector sum of forces on certain object is the product of the mass of that object and the acceleration vector of the object. Based on the Newton's second law of motion, two governing equations are generated which can describe the motion of LCM particle in horizontal and vertical directions:

$$D_x = \frac{m_m dv_x}{g_c dt}, \quad (\text{B.1})$$

$$W - B - D_y = \frac{m_m dv_y}{g_c dt}, \quad (\text{B.2})$$

where

B buoyant force, lbf

D_x viscous drag in the horizontal direction, lbf

D_y viscous drag force in the vertical direction, lbf

$g_c 32.17$ (ft-lb_m/lb_f-s²) = unit conversion factor

m_m LCM mass, lbm

WLCM weight, lbf

The drag force can be expressed as [28]:

$$D = f A E_k, \quad (\text{B.3})$$

where E_k is the kinetic energy per unit volume. For vertical settling motion, the E_k is defined as

$$E_k = \frac{\rho_f v_y^2}{2g_c}, \quad (\text{B.4})$$

where v_y is the velocity of LCM in vertical direction; ρ_f is the density of the drilling fluid; g_c is the unit conversion factor, which is equal to 32.17.

For horizontal drifting motion, the E_k is defined as

$$E_k = \frac{\rho_f (v_L - v_x)^2}{2g_c}, \quad (\text{B.5})$$

where v_x is the velocity of LCM particle in horizontal direction; v_L is the velocity of drilling fluid; ρ_f is the density of the drilling fluid; g_c is the unit conversion factor, which is equal to 32.17.

The friction factor f can be calculated as a function of the Reynolds number and LCM particle sphericity. Fang and Guo [29] developed the following correlations:

$$f = 10 \wedge \left(A' + B' \log(N_{\text{Re}}) + C' [\log(N_{\text{Re}})]^2 \right), \quad (\text{B.6})$$

where

$$A' = 2.2954 - 2.2626\psi + 4.4395\psi^2 - 2.9825\psi^3, \quad (\text{B.7})$$

$$B' = -0.4193 - 1.9014\psi + 3.3416\psi^2 - 2.0409\psi^3, \quad (\text{B.8})$$

$$C' = 0.1117 + 0.0553\psi - 0.1468\psi^2 + 0.1145\psi^3, \quad (\text{B.9})$$

where ψ is the sphericity of LCM particle and N_{Re} is the Reynolds number of LCM particle.

For vertical settling, the Reynolds number is defined by

$$N_{\text{Re}} = \frac{124\rho_f v_y d_m}{\mu}, \quad (\text{B.10})$$

where ρ_f is the density of the drilling fluid; v_y is the velocity of LCM in vertical direction; d_m is the equivalent diameter of particle; μ is the drilling fluid viscosity.

For horizontal drifting, the Reynolds number is defined by

$$N_{\text{Re}} = \frac{124\rho_f (v_L - v_x) d_m}{\mu}, \quad (\text{B.11})$$

where ρ_f is the density of the drilling fluid; v_L is the velocity of drilling fluid; v_x is the velocity of LCM in horizontal direction; d_m is the equivalent diameter of particle; μ is the drilling fluid viscosity.

Integrating Equation (B.2) with the initial condition of $v_y = v_o \cos(\delta) = v_{yo}$ gives

$$v_y = \frac{\sqrt{W-B}}{\beta} \left(\frac{C_y - e^{-at}}{C_y + e^{-at}} \right), \quad (\text{B.12})$$

where

$$\alpha = \frac{2g_c \beta}{m_m} \sqrt{W-B}, \quad (\text{B.13})$$

$$\beta = \sqrt{\frac{fA\rho_m}{2g_c}}, \quad (\text{B.14})$$

$$C_y = \frac{\sqrt{W-B} + v_{yo}\beta}{\sqrt{W-B} - v_{yo}\beta}, \quad (\text{B.15})$$

Denoting $v_y = dy/dt$ and integrating Equation (B.12) with the initial condition of $y = 0$ yields

$$y = \frac{1}{\beta} \sqrt{W-B} \left[t + \frac{2}{\alpha} \ln \left(\frac{C_y + e^{-at}}{C_y + 1} \right) \right]. \quad (\text{B.16})$$

Integrating Equation (B.1) with the initial condition of $v_x = v_o \sin(\delta) = v_{xo}$ gives

$$v_x = v_L - \frac{2m_m}{fA\rho_f(t + C_x)}, \quad (\text{B.17})$$

where

$$C_x = \frac{2m_m}{fA\rho_f(v_L - v_{xo})}. \quad (\text{B.18})$$

Denoting $v_x = dx/dt$ and integrating Equation (B.17) with the initial condition of $x = 0$ gives

$$x = v_L t + \frac{2m_m}{fA\rho_f} \ln \left(\frac{C_x}{t + C_x} \right). \quad (\text{B.19})$$

The values of parameters in the mathematical model can be determined as follows:

$$A = \frac{1}{4} \pi \left(\frac{d_m}{12} \right)^2, \quad (\text{B.20})$$

$$B = \frac{g}{g_c} \rho_f V_m, \quad (\text{B.21})$$

$$W = \frac{g}{g_c} \rho_m V_m, \quad (\text{B.22})$$

$$m_m = \rho_m V_m, \quad (\text{B.23})$$

$$V_m = \frac{1}{6} \pi \left(\frac{d_m}{12} \right)^3, \quad (\text{B.24})$$

where ρ_m is the LCM density; ρ_f is the density of the drilling fluid; d_m is the equivalent diameter of particle; g is the gravitational acceleration; g_c is the unit conversion factor, which is equal to 32.17.

The friction factor is not sensitive to the particle Reynolds number but to the particle sphericity for large cuttings sizes

and high fluid velocities. Therefore, friction factor can be assigned constant values.

Nomenclature

A : Characteristic area of LCM particle, ft^2
 A' : Defined by Equation (B.7)
 B : Buoyant force, lbf
 B' : Defined by Equation (B.8)
 C' : Defined by Equation (B.9)
 D : Viscous drag force, lbf
 D_e : Equivalent diameter of the fracture area, m
 d_m : Equivalent diameter of LCM particle, in.
 D_x : Viscous drag force in the horizontal direction, lbf
 D_y : Viscous drag force in the vertical direction, lbf
 E_k : Kinetic energy per unit volume, $\text{blf-ft}/\text{ft}^3$
 f : Friction factor
 f_{vi} : Weight fraction of LCM size d_{mi}
 g : $32.17 \text{ ft/s}^2 = \text{gravitational acceleration}$
 g_c : $32.17 (\text{ft-lb}_m/\text{lb}_f\text{-s}^2) = \text{unit conversion factor}$
 h : Height of LCM slice, ft
 h_f : Height of fracture in lost circulation model, m
 h_L : Height of the liquid column, m
 H_f : Height of fracture in plugging model, ft
 i : Index for slice number
 k_f : Fracture permeability, Darcy
 L_f : Invaded fracture length, m
 m_m : LCM mass, lbm
 N : Number of slices
 N_{Re} : Reynolds number of LCM particle
 p_w : Borehole pressure, KPa
 p_f : Fracture pressure, KPa
 T : Thickness of LCM slice, ft
 V : Volume of LCM slice, ft^3
 V_m : LCM particle volume, ft^3
 V_t : Total volume of LCM pile, ft^3
 V_L : Cumulative volume of lost liquid for two wings, m^3
 v_L : Drilling fluid velocity, ft/s
 v : Velocity of drilling fluid, m/s
 v_o : Initial LCM velocity, ft/s
 v_x : LCM velocity in x -direction, ft/s
 v_{xo} : Initial LCM velocity in x -direction, ft/s
 v_y : LCM velocity in y -direction, ft/s
 v_{yo} : Initial LCM velocity in y -direction, ft/s
 W : Weight of LCM particle, lbf
 w : Width of fracture, m
 ω : Width of LCM slice, ft
 x : LCM drifting distance in the fluid flowing direction, ft
 X : Distance that the fluid flows, cm
 y : LCM settling distance in the vertical direction, ft

Greeks

ψ : Particle sphericity
 μ : Drilling fluid viscosity, cp
 ρ_L : Drilling fluid density, kg/m^3
 ρ_f : Drilling fluid density, lbm/ft^3

ρ_m : LCM density, lbm/ft^3
 q : Drilling fluid loss rate, m^3/s
 q_L : drilling fluid loss rate into one fracture wing, m^3/s

Data Availability

The data used to support the findings of this study are included within the article.

Conflicts of Interest

The authors declare that they have no conflicts of interest.

References

- [1] H. Wang, *Near Wellbore Stress Analysis for Wellbore Strengthening*, PhD Dissertation. University of Wyoming, Laramie, WY, USA, 2007.
- [2] J. Cook, F. Growcock, Q. Guo, M. Hodder, and E. Van Oort, "Stabilizing the wellbore to prevent lost circulation," *Oilfield Review*, vol. 23, pp. 26–35, 2011.
- [3] R. Majidi, S. Z. Miskaand, and M. Yu, "Modeling of drilling fluid losses in naturally fractured formations," in *SPE Annual Technical conference and Exhibition*, Denver, Colorado, USA, 2008b.
- [4] R. Majidi, S. Z. Miska, and L. G. Thompson, "Quantitative analysis of mud losses in naturally fractured reservoirs: the effect of rheology," in *SPE Western regional and pacific Section AAPG Joint Meeting*, Bakersfield, California, USA, 2008a.
- [5] D. Li, Y. Kang, and X. Liu, "The lost circulation pressure of carbonate formations on the basis of leakage mechanisms," *Acta Petrolei Sinica*, vol. 32, pp. 900–904, 2011.
- [6] M. Wang, Y. Guo, M. Fangand, and S. Zhang, "Dynamics simulation and laws of drilling fluid loss in fractured formations," *Acta Petrolei Sinica*, vol. 38, pp. 597–606, 2017.
- [7] Y. Feng and K. E. Gray, "Modeling lost circulation through drilling-induced fractures," *SPE Journal*, vol. 23, pp. 205–223, 2017.
- [8] M. W. Sanders, J. T. Scorsone, and J. E. Friedheim, "High-fluid-loss, high-strength lost circulation treatments," in *SPE Deepwater Drilling and Completions Conference*, Galveston, TX, USA, 2010.
- [9] J. Castro, L. Solis, J. A. Urdaneta, and J. V. A. Morales, "First application of heat-activated, rigid rapid-fluid system in deep-water environment in Mexico helps to cure severe loss of circulation: a case history," in *SPE/IADC Drilling Conference and Exhibition*, Amsterdam, The Netherlands, 2011.
- [10] A. Ay, I. H. Gucuyener, and M. V. Kok, "An experimental study of silicat-polymer gel systems to seal shallow water flow and lost circulation zones in top hole drilling," *Journal of Petroleum Science and Engineering*, vol. 122, pp. 290–699, 2014.
- [11] P. Zhao, C. L. Santana, Y. Feng, and K. E. Gray, "Mitigating lost circulation: a numerical assessment of wellbore strengthening," *Journal of Petroleum Science and Engineering*, vol. 157, pp. 657–670, 2017.
- [12] A. Mehrabian and Y. Abouseiman, "Wellbore geomechanics of extended drilling margin and engineered lost-circulation solutions," *SPE Journal*, vol. 22, no. 4, pp. 1178–1188, 2017.
- [13] S. Abdila, A. Harahap, and H. Yuristyanto, "Casing drilling technology as the solution for severe lost circulation: LSE

- casing drilling pilot project case study,” in *IADC/SPE Asia Pacific Drilling Technology Conference*, Bangkok, Thailand, 2018.
- [14] X. Hou, J. Yang, Q. Yin et al., “Lost circulation prediction in south China sea using machine learning and big data technology,” in *Offshore Technology Conference*, Houston, Texas, 2020.
- [15] D. Pazziuagan, A. Giles, and J. Martin, “A field-proven wellbore strengthening method for helping prevent lost circulation in highly depleted mature fields: ultra-deepwater Gulf of Mexico,” in *Offshore Technology Conference*, Houston, Texas, 2020.
- [16] Y. Feng and K. E. Gray, “Review of fundamental studies on lost circulation and wellbore strengthening,” *Journal of Petroleum Science and Engineering*, vol. 152, pp. 511–522, 2017.
- [17] S. Kefi, J. C. Lee, N. D. Shindgikaret, C. Brunet-Cambus, B. Vidick, and N. I. Diaz, “Optimizing in four steps composite lost-circulation pills without knowing loss zone width,” in *IADC/SPE Asia Pacific Drilling Technology Conference and Exhibition*, Ho Chi Minh City, Vietnam, 2010.
- [18] S. M. Javeri, Z. W. Haindade, and C. B. Jere, “Mitigating loss circulation and differential sticking problems using silicon nanoparticles,” in *Middle East Drilling Technology Conference and Exhibition*, Muscat, Oman, 2011.
- [19] H. Guo, J. Voncken, T. Opstal, R. Dams, and P. L. J. Zitha, “Investigation of the mitigation of lost circulation in oil-based drilling fluids by use of gilsonite,” *SPE Journal*, vol. 19, pp. 1–184, 2014.
- [20] S. Savari, D. L. Whifill, D. E. Jamison, and A. Kumar, “A method to evaluate lost-circulation materials—investigation of effective wellbore-strengthening applications,” *SPE Drill Completion*, vol. 29, no. 3, pp. 329–333, 2014.
- [21] O. Razavi, A. K. Vajargah, E. van Oort, M. Aldin, and S. Govindarajan, “Optimum particle size distribution design for lost circulation control and wellbore strengthening,” *Journal of Natural Gas Science and Engineering*, vol. 35, pp. 836–850, 2016.
- [22] A. Nasiri, A. Ghaffarkhah, M. K. Moraveji, A. Gharbanian, and M. Valizadeh, “Experimental and field test analysis of different loss control materials for combating lost circulation in bentonite mud,” *Journal of Natural Gas Science and Engineering*, vol. 44, pp. 1–8, 2017.
- [23] S. D. Kulkarni, D. E. Jamison, and K. D. Teke, “Managing suspension characteristics of lost-circulation materials in a drilling fluid,” *SPE Drilling & Completion*, vol. 30, pp. 310–315, 2015.
- [24] M. Jaffery, A. Wicaksono, M. Pasteris, M. Subhan, B. Amir, and M. Mansur, “Case study—engineered fiber-based loss circulation control pills EFLCC solves total loss circulation challenges on complex depleted and fractured formation in Natuna Sea, Indonesia,” in *Offshore Technology Conference Asia*, Kuala Lumpur, Malaysia, 2016.
- [25] C. Xu, J. Zhang, Y. Kang et al., “Investigation on the transport and capture behaviours of lost circulation material in fracture with rough surface,” in *International Petroleum Technology Conference*, Beijing, China, 2019.
- [26] S. Savari and D. L. Whitfill, “Managing lost circulation in highly fractured, vugular formations: engineering the LCM design and application,” in *Abu Dhabi International Petroleum Exhibition & Conference*, Abu Dhabi, UAE, 2019.
- [27] Y. Feng, G. Li, and R. Li, “Influence of the lost circulation material injection method on the fracture plugging: a visualization experimental study,” in *Unconventional Resources Technology Conference*, Virtual, 2020.
- [28] T. A. Bourgoyne, E. M. Chenevert, K. K. Millhein, and F. S. Young, “Applied drilling engineering,” in *SPE Textbook Series*, pp. 173–175, Richardson, TX, USA, 1986.
- [29] Q. Fang, B. Guo, and A. Ghalambor, “Formation of underwater cuttings piles in offshore drilling,” *SPE Drilling & Completion*, vol. 23, no. 1, pp. 23–28, 2008.